Received: 7 May 2020 | Revised: 25 July 2020 | Accepted: 17 August 2020

DOI: 10.1111/coin.12406

SPECIAL ISSUE ARTICLE

Computational Intelligence WILEY

An experimental approach to evaluate machine learning models for the estimation of load distribution on suspension bridge using FBG sensors and IoT

Ambarish G. Mohapatra[1] | **Ashish Khanna**[2] | **Deepak Gupta**[2] | **Maitri Mohanty**[3] | **Victor Hugo C. de Albuquerque**[4]

[1]Department of Electronics and Instrumentation Engineering, Silicon Institute of Technology, Bhubaneswar, India

[2]Maharaja Agrasen Institute of Technology, Delhi, India

[3]Computer Science & Engineering, GIET University, Gunupur, India

[4]Graduate Program in Applied Informatics, University of Fortaleza, Fortaleza, Brazil

Correspondence
Ambarish G. Mohapatra, Department of Electronics and Instrumentation Engineering, Silicon Institute of Technology, Bhubaneswar, India.
Email: ambarish.mohapatra@gmail.com
Deepak Gupta, Computer Science & Engineering, GIET University, Gunupur, Odisha, India.
Email: deepakgupta@mait.ac.in

Funding information
TEQIP-III BPUT Collaborative Research and Innovation Scheme (CRIS) and Silicon Research Promotion Scheme (SRPS)

Abstract

Most of the tragedies on any bridge structure have been the cause of high-density crowd behavior as a response to trampling as well as the crushing scenario. Therefore, it is most important to monitor such unforeseen situations by sensing the load imposed on the bridge structures. This scenario may arise where crowd movement is huge on these types of bridges. Similarly, the fiber Bragg grating (FBG) is a promising technology for structural health monitoring applications. In this work, an Internet of Things based FBG optical sensing scheme is proposed to monitor real-time strain distribution throughout the bridge structures and localization of load imposed on the structure from a central control room. A suspension bridge model is designed by referring to a real bridge scenario and these FBG sensors are deployed to validate the proposed machine learning models. In this article, the performances of two machine learning strategies are discussed for the accurate estimation of load and its position by acquiring high sensitive FBG sensors signals at a very high data rate. The algorithms include K-nearest neighbor (KNN) and random forest (RF); which are applied on each sensing data source, and then validated using a prototype sus-

pension bridge model integrated with three FBG sensors (1532 nm, 1538 nm, and1541 nm) on a single optical fiber cable.

KEYWORDS

FBG Sensor, Internet of Things, K-Nearest Neighbor, Random Forest, Structural Health Monitoring

1 | INTRODUCTION

Fiber Bragg gratings (FBGs) are used as passive optical sensors for various purposes like structural health monitoring (SHM), biomedical sensors, chemical sensors, sensors in aerospace applications where EM radiation may create abnormalities during measurement. These sensors can be used to measure various measurands like strain, displacement, velocity, acceleration, vibration, tilt angle, and so on. These FBG sensors are primarily sensitive to the effect of strain on the grating region. Various transduction principles are used to convert the effect of strain change into other physical sensing mechanisms like strain change to displacement and effect of dynamic strain to vibration measurement.[1] These FBG sensors are capable to sense very minimum strain and temperature change of resolution about 0.4μstrain and 0.05°C, respectively. The commercial FBG sensors are having strain sensitivity of 1.2 pm/μstrain and 11 pm/°C, respectively.[2–4]

An FBG-based sensor offers various other advantages over other electronic sensors such as immunity to EMI radiation, high sensitivity, multiplexing, as well as distributed sensing capacity.[1,2,5–7] In a similar context, the Internet of Things (IoT)-based distributed sensing approach will provide better scalability compared with an offline monitoring mechanism.[8–10] Thereby, FBG sensing systems can be integrated into an IoT framework for better signal processing, historical data management, scalable solutions, and smart decision support along with notification generations. These systems have added advantages to provide a complete monitoring, processing, and notification (MPN) approach where cross-platform service is not an issue. The major benefit is to connect a large volume of users to the proposed sensing system through smart devices like Android/IOS devices and tablets.

This article comprises the other five sections such as literature review on FBG sensors, experimental setup, proposed methodology, result analysis of the proposed methodology, and conclusion.

A detailed literature review is discussed in the second section of this article. The focus of this literature review is to perform a study on different experimental works published in the various research articles to date. Furthermore, the implementation of a test case on the experimental work is discussed in this third section. Similarly, the fourth and fifth sections of this article give a result-based analysis between two proposed machine learning models for the analysis of structural parameters such as load distribution and localization technique. The other interest of this proposed framework is to share the knowledge on the design of an indigenous experimental prototype for the testing of different SHM applications.

2 | LITERATURE REVIEW

The literature review is formed on two aspects of the SHM experimentations such as the deployment of sensors on the experimental testbed and the evaluation of effective machine learning models for the analysis of load flow on the structure.

First, a detailed study is done on the various types of optical sensors and optical sensing schemes reported to date for the measurement of several physical quantities such as displacement, velocity, tilt angle, cracks, pressure, and so on.

Several research articles are published on the architecture of remote measurement schemes in SHM applications. The usage of FBG sensors and connecting FGB sensing systems to IoT environments in SHM applications are not much explored. Similarly, IoT is an emerging field of research as data velocity, data variety, data volume, and data securities are the major concerns of all researchers. The FBG sensing mechanisms are not cost-effective solutions in every application, but it is mostly preferred as the speed of measurement, site maintenance, and dynamic analysis of structures is never been a problem for the industries. The machine learning models can be fitted to the IoT models for the monitoring of real-time SHM information remotely from a control station. Rekha et al (2018) have proposed wireless sensor network (WSN) based SHM framework and the decision support mechanism to generate adequate notifications for the authorities.[11] In the article, Rekha et al (2018), a wireless sensor network (WSN) based experiment was conducted to collect real-time data from the structure. The state monitoring and reporting mechanism were proposed in this work. The complete system was designed using WSN and smartphone android application. The proposed system utilizes electronic sensors and the data collection is performed as static measuring quantities. Continuous signal recording using high speed and high accuracy based sensors; data analysis and decision support system (DSS) based approaches are not discussed in this article. Furthermore, the speed of data acquisition is not discussed in the above article.[11] Apart from the above aspects, it is obvious that the sensitivity of conventional sensors in the WSN techniques cannot match the sensitivity and resolution of FBG sensing mechanisms.

Similarly, the article published by Yasuda and Miyazaki (2017) portrayed structural integrity F-test (SI-F) for the monitoring of fatigue crack in a structure. The strain distribution was also evaluated using finite element analysis (FEA) of the same structure. The real-time sensor data were collected from a WSN model connected to a cloud infrastructure using the 3G network. In this research article, a fatigue crack of 20 mm length and 3 mm depth was successfully detected using conventional strain sensors.[12] These conventional sensors are not capable to detect very small cracks less than 20 mm length and 3 mm depth.

Alavi and Buttlar (2019) have presented a detailed literature review on smartphone-based monitoring of civil structures. In a similar context, a case study on the deployment of VDO cameras in the civil structures is presented in a detailed manner. The detection is a very small pothole that is not possible to detect in the current scenario and also the DSS based models are not discussed in this article. Historical data management is also discussed in the article.[13] Machine learning has been applied for IoT privacy,[14] security,[15,16] healthcare,[17] intelligent transport systems,[18] and IoT devices.[19]

Mustapha et al (2020) have proposed two machine learning models for the estimation of crowd flow on a bridge structure. They have shown a sensor fusion technique by employing FBG sensing and inertial measurement units (IMUs) for the estimation of crowd flow. The estimation models proposed in this article are convolutional neural networks (CNN) and support vector machines (SVM).[20] The proposed technique is based on a conventional sensor-based structural monitoring application to monitor the real-time status of the crowd flow on the bridge structure.

Bao et al (2019) have presented an anomaly diagnosis approach using a deep learning model, computer vision-based crack identification model, and machine learning-based condition assessment approach for the bridge structure. This article provides a brief technological utilization of different methodologies for the SHM application. This article shows a computational approach to identify certain aspects of SHM technology. On the other hand, the sensing scheme is not discussed in the article. The testing is performed by the simulated data set generated using computation modeling.[21]

Similarly, Li et al (2019) proposed a theoretical sensing scheme using finite element analysis (FEA) and an experimental test case to validate the theoretical model. Two FBG sensors are developed with an overall sensitivity of 7.72 and −2.94 pm/με, respectively. The overall sensitivities are 6.43 and −2.45 times of the strain sensitivity of a bare FBG sensor. These sensors are most suitable in varying temperature environments for critical mechanical types of equipment.[22] The article Li et al (2019), shows the design and development of the sensor only, and the data acquisition, signal processing, and analysis are not discussed.

Furthermore, many research reports have been published on the FBG sensing mechanism in SHM applications. There are various kinds of research works published until now. Some works are based on the development of good accuracy based FBG sensors, calibration models for FBG sensors, localization of fractures, and development of novel sensors for pressure, temperature, soil strength, air particle monitoring. Few research articles are listed in Table 1 which depicts the novelty approach of the proposed sensing mechanism.

In a similar context, the development of new FBG sensors and sensing methodologies are studied in this section. The relevant studies are listed in Table 2 where different FBG sensing mechanisms used in SHM applications are discussed with their advantages. From the above review, it is summarized that the SHM application covers a wide variety of technological challenges and there are many verticals in the SHM based strategies. The generic view of the structural health monitoring (SHM) is portrayed in Figure 1 where various technological aspects are shown. The FBG sensor-based SHM application comes in the first category of the list shown in Figure 1. The above review is performed to gather parametric performance evacuation of various SHM applications and technological comparisons.

It is observed from the review that various types of technologies are used to perform SHM applications such as WSN, IoT, and soft approaches. On the other hand, the load analysis using FBG sensing technology and IoT-driven decision support system are not much discussed together in most of the research articles. These two research aspects are discussed in this article in a detailed manner and the experimental setup is also presented in this work. The further section of the article discusses the components used in the experimental setup, real-time signal recording from the test suspension bridge model, machine learning models to predict the load and position using three FBGs distributed on one section of the bridge model, IoT-based decision support model.

3 | EXPERIMENTAL SETUP

Three FBG sensors are bonded to the deck of the suspension bridge model consisting of gray cast iron material having a tensile strength of 170 MPa. The stress, strain, and maximum deformation of the suspension bridge model are analyzed using ANSYS finite element analysis (FEA) technique. It is observed that the regions of the deck near-vertical support are exposed to maximum strain and the center region of the deck is exposed to maximum deformation during gravitational

TABLE 1 Some of the research highlighted on FBG sensor in SHM applications

Author	Proposed methodology	Key findings
Yu et al (2018)	Proposed a low-velocity impact methodology using detrended fluctuation analysis and centroid localization algorithm for SHM application[23]	Presented the average error of localization about 31.5 mm using the proposed methodology
Mieloszyk and Ostachowicz (2017)	SHM was implemented on a wind turbine model to detect the damage and localize it[24]	Identified the location of the damage
Li et al (2019)	Discussed fiber Bragg grating (FBG) demodulator based tunable lasers used for SHM applications. Sensor accuracy was also discussed[25]	The improvement scheme of FBG interrogation accuracy from ±3 pm to ±1 pm was proposed
Tahar et al (2017)	Proposed a fiber Bragg grating sensors (FBGS) based on wireless sensor technology for the measurement of strain and temperature in structural health monitoring applications[25]	An efficient method to accurately measure the variations of strain, temperature, and humidity by developing a model using FBG sensing technology
Sindagi et al (2018)	Discussed the crowd monitoring and estimation using the support vector machine (SVM) and neural network (NN) based approach[26]	The crowd tackling and danger notification using the decision support system approach is presented
Zhan et al (2008)	Presented advanced computer vision-based method to study the crowd movement. The crowd density is also discussed[27]	Face recognition, head, and pedestrian movement tracking is presented
Zhang et al (2016)	Discussed a multi-column-based convolutional neural network (CNN) model to locate the density using image processing technique[28]	Local density and people per square meter are estimated using the proposed methodology.
Sindagi et al (2017)	Proposed a crowd count classification model and various density levels are presented using the image processing technique[29]	The proposed model classifies the crowd level from the image into different density levels
Jiao et al (2018)	Presented a multisensor data through CNN based multisensor golf swing classification. They have used sensors such as accelerometers, gyroscopes, and strain gauges[30]	A smart golf club integrated solution is proposed in the research
Alavi and Buttlar (2019)	Discussed a smartphone-based structural health monitoring application and communication technologies with sensors[31]	The installation scheme and estimated cost factor are presented in the article

TABLE 2 Research and development on FBG sensing schemes in SHM applications

Author	Proposed methodology	Key findings
Li et al (2019)	Two FBG sensors are developed with an overall sensitivity of 7.72 pm/με and −2.94 pm/με, respectively[22]	The overall sensitivities are 6.43 and −2.45 times of the strain sensitivity of a bare FBG sensor
Koerdt et al (2016)	The optical, thermomechanical, and mechanical characterization of an ultraviolet laser-based generation of Bragg gratings in a perfluorinated polymer optical fiber (POF) is performed[50]	It is observed that the polymer optical fibers are feasible in contrast to glass optical fibers. The results are also promising regarding stability and reliability
Zheng et al (2018)	In this study, the structural adhesive was used to join the FBGs with steel wire, and the relevant measurability and reliability of the adhesive-bonded FBGs with steel wire were investigated by loading and unloading cyclic test and fatigue test in the application of FBGs to monitor bridge cable force[51]	It was found that there was a linear relationship between the load and the wavelength for both the loading and the unloading phases, and the data line from the loading process was parallel to that of the unloading process

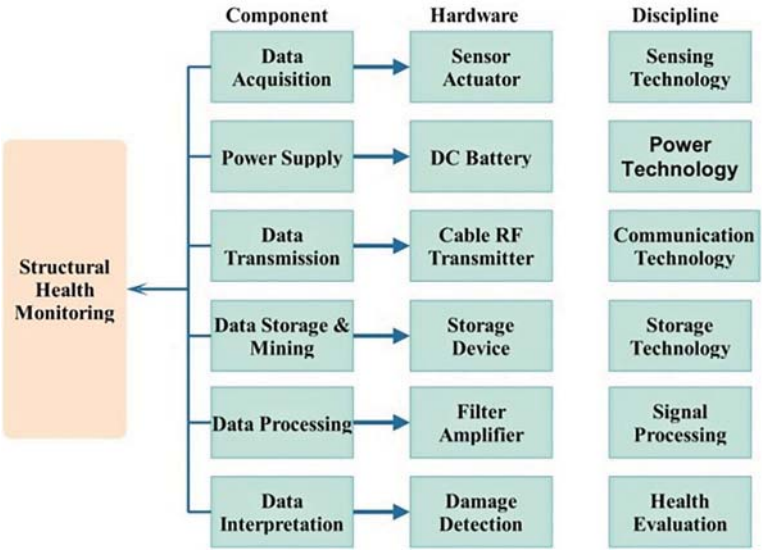

FIGURE 1 Generic technological aspects of SHM applications [Color figure can be viewed at wileyonlinelibrary.com]

load. Therefore, three specific positions are chosen to fix the FBG sensors (1532, 1538, 1541 nm) for real-time data recording. The sensor positions are marked in Figure 2A where a one-half section of the bridge model is considered to have experimented as the other half is similar to the first one. During data recording, five individual positions are considered where the loads in kilograms are applied for the testing of prediction algorithms.

First, the sensors are fabricated at CGCRI, Kolkata, India using a femtosecond laser direct-writing system (femtoFBG writing system). The sensors are interfaced with Ibsen IMON

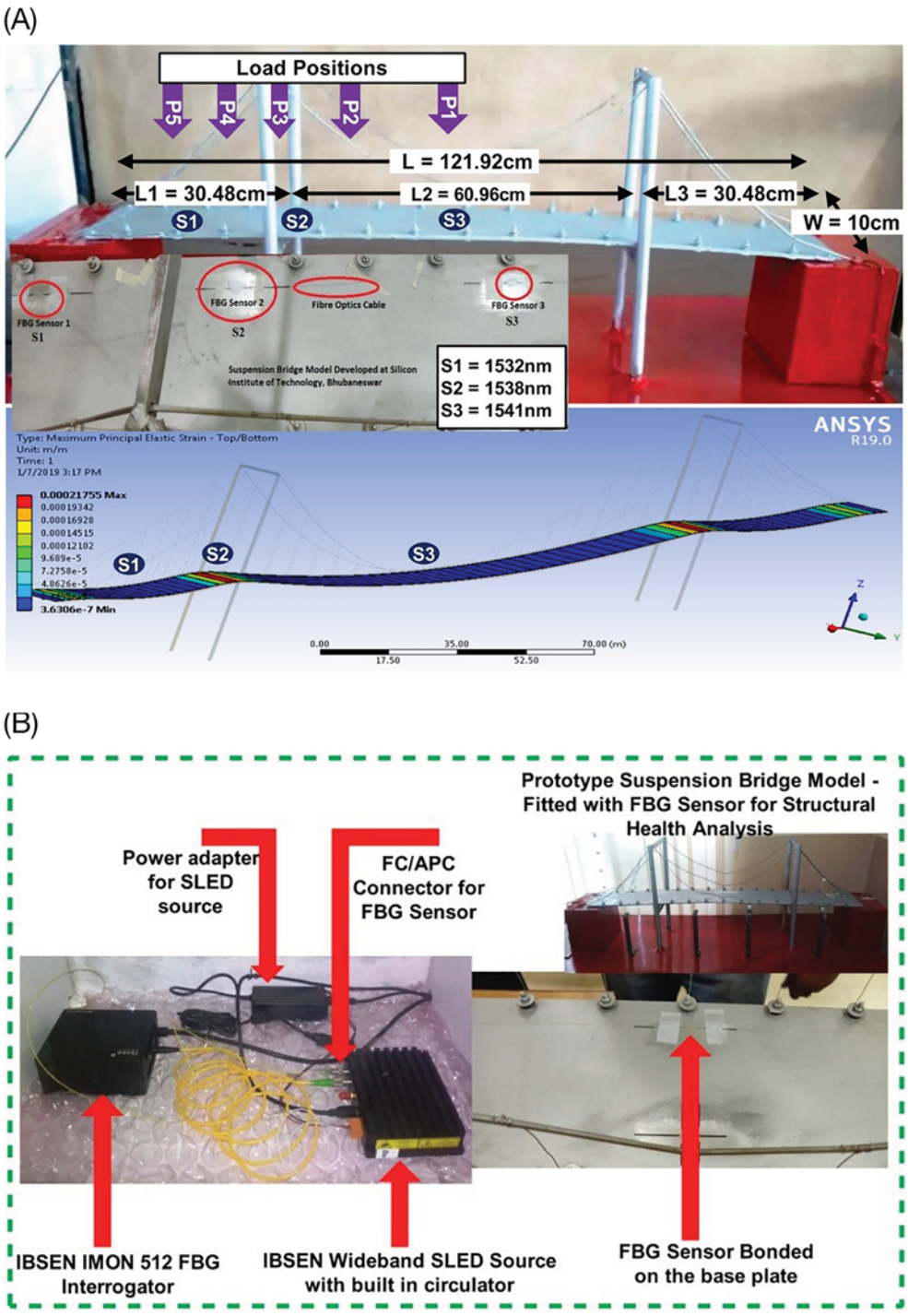

FIGURE 2 A, Experimental setup of the prototype suspension bridge structure, FBG sensors, and FEA model using ANSYS. B, Experimental setup of the FBG Sensor Interrogation unit with SLED light source [Color figure can be viewed at wileyonlinelibrary.com]

512 High-speed FBG interrogator, Ibsen SLED light source, and the signal acquisition is performed via LAN interface with the host PC. Furthermore, the wavelength shift is recorded using IMON 512 FBG Interrogator (1528-1568 nm, 2.5 kHz) to develop the load estimation and localization model.

The data acquisition is performed using the LabVIEW DLL library file supplied by the vendor. The complete experimental setup is shown in Figure 2A where the dimensions of the bridge model and the strain distribution profile obtained from the FEA model are also portrayed. The experimental setup for the Interrogation unit with SLED wideband light source is shown in Figure 2B.

4 | PROPOSED METHODOLOGY

The FBG sensors are characterized by the Bragg wavelength (λ_B) which is sensitive to temperature and strain change. According to the FBGs characteristic sensing principle, the Bragg wavelength shifts with the change in exposed temperature and strain. The FBGs fabrication process is an expensive and highly precise methodology.[32–34] According to coupled-mode theory, the Bragg wavelength (λ_B) is closely related to the effective refractive index (n_{eff}) and FBG period (Λ) as per Equation (1).

$$\lambda_B = 2n_{eff}\Lambda. \tag{1}$$

In summary, the central reflection wavelength shift ($\Delta\lambda_B$) of the Bragg sensor is affected by temperature (ΔT) and strain (ε), the relationship between these physical parameters is given by Equation (2).

$$\frac{\Delta\lambda_B}{\lambda_B} = (1-\rho_e)\varepsilon + (\propto +\xi)\Delta T. \tag{2}$$

In Equation (2), the parameters such as ρ_e, $\propto$, and ξ are the photoelastic coefficients, thermal expansion coefficient, and thermo-optic coefficient, respectively. Furthermore, the gauge factor (G) of the FBG strain sensor can also be represented as in Equation (3).[32,34,36]

$$G = (1-\rho_e) * (\lambda_B/1e6). \tag{3}$$

Similarly, the reflection and transmission of FBG sensor concerning the wavelength (λ) can be formulated as in Equations (4) and (5), respectively.

$$r(\lambda) = \frac{iKsinh(QL)}{Qcosh(QL) - i\Delta\beta\sinh(QL)}, \tag{4}$$

$$t(\lambda) = \frac{Q}{Qcosh(QL) - i\Delta\beta\sinh(QL)}, \tag{5}$$

where $Q(\lambda) = \sqrt{|K|^2 - |\Delta\beta|^2}$.

The coupling strength is represented by $K(\lambda) = (\Delta n\pi)/\lambda$, where Δn is the index modulation and L is the grating length. $\Delta\beta = (2\pi n_{eff})(\lambda^{-1} - \lambda_B{}^{-1})$ is the phase mismatch. The above

parameters will allow calculating the transmission and reflection of the FBG sensor. The above equations represent the grating wavelength (λ_B) is closely related to the strain input supplied to the FBGs. Alternatively, to use stress instead of strain (for anisotropic material), the relationship between several stress components can be mathematically represented as in Equation (6).[32–36]

$$\varepsilon = \frac{1}{E}(\sigma_{zz} + \nu\sigma_{xx} + \nu\sigma_{yy}), \tag{6}$$

where E is Young's modulus of elasticity and ν is the poison's ratio of the FBG core-cladding material. These are the average value of the FBG core-cladding compound. Similarly, σ_{xx}, σ_{yy} are the transverse stresses and σ_{zz} is the longitudinal stress component. From Equations (4) and (5), it is observed that the reflected and transmitted wavelengths from the FBG sensor are just a mirror image to each other. The received power (P) at the photodetector after transmitting twice through 3 dB coupler, the power can be represented as in Equation (7). The incident light power per unit wavelength is represented as I_o.

$$P(\lambda) = I_o \int_{-\infty}^{+\infty} r(\lambda)\, t(\lambda) d\lambda. \tag{7}$$

The experiment is carried out by applying different loads (in kilograms) at the predefined positions of the suspension bridge structure and further, the wavelength shifts due to applied load are recorded for the implementation of the proposed estimation model. The complete block diagram of the proposed methodology for the proper estimation of the applied load and position on the bridge structure is shown in Figure 3. Two estimation models such as K-nearest neighbor (KNN) and random forest (RF) are tested during the experiment. The accuracy, mean square error (MSE), root mean square error (RMSE), and R-squared value of each model are calculated to summarize the best possible method for this application. The configuration settings and analytical modeling behind the above distinct steps are explained in the subsequent subsections.

4.1 | Moving average filter

The moving average filter is the most commonly adopted and easily developed signal filtering mechanism in almost all the DSP applications. This filtering mechanism is an optimal filtering scheme for reducing random noise while retaining a sharp step response. Due to this advantage, it is widely used in most of the common time-domain filtering schemes but it is having a very bad reputation in frequency domain filtering due to its inability to separate one band of frequencies from another. There are other filtering approaches are available such as Gaussian, multiple-pass moving average, and Blackman filter. These filtering schemes are having better performance in the frequency domain but the computation time is quite high due to its complexity. In this work, we have utilized a moving average filter of window size of 80 and the filtered signal "y(n)" is estimated as shown in Equation (8) where the input signal is represented as "x(n)."

$$y(n) = \left({}^{1}/_{window_{size}}\right)[x(n) + x(n-1) + \ \ldots\ + x(n-(window_{size}-1))]. \tag{8}$$

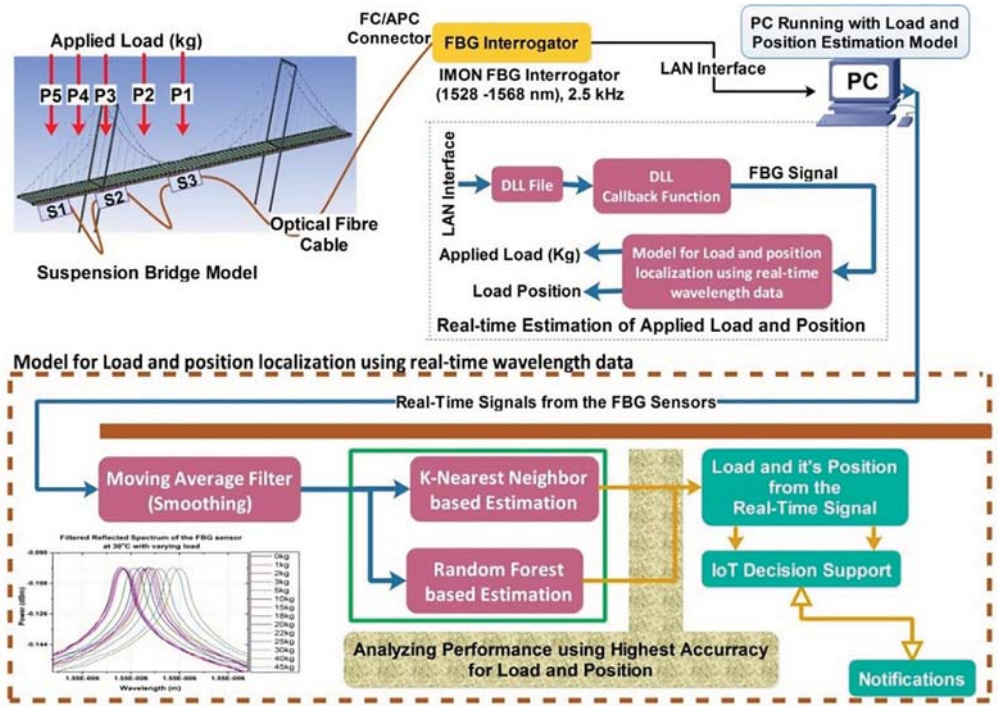

FIGURE 3 Block diagram of the proposed methodology and flow model [Color figure can be viewed at wileyonlinelibrary.com]

4.2 | K-nearest neighbor (KNN) model

The KNN technique is widely used in various machine learning applications. This algorithm is a supervised learning methodology and it is a nonparametric algorithm.[37,38] This is also called a lazy learner algorithm where it does not learn from the training data set immediately. The basic principle of this technique is based on the classification of training data sets when it founds new data as input.[39] This KNN algorithm is chosen to be fitted for our application because the signal from the FBG sensor is always noisy and the data set is very large when more number of sensors will be fitted to such SHM applications. Apart from that, this method is a simple training approach and the implementation is easy. The training of KNN model solely depends on the best suitable value of "k" and the training performance is often better when the "k" is large.[37–40] The pseudo-code of the KNN algorithm used in this article is shown below.

Step 1: Choose the number of K of the neighbours

Step 2: Evaluate the Euclidean distance of the K number of neighbours

The Euclidean distance between two points A and B having coordinates (X_1, Y_1) *and* (X_2, Y_2) respectively can be represented as

$$\sqrt{(X_2 - X_1)^2 + (Y_2 - Y_1)^2}$$

Step 3: Select the K nearest neighbours as per the Euclidean distance

Step 4: Count the number of datasets among these K number of neighbours in each category

Step 5: Assign the new data point to the category where the number of neighbours are maximum

In this application, we have considered k = 10 as this gives better accuracy for predicting load and position values from the sensor wavelength shifts.

4.3 | Random forest (RF) model

The random forest algorithm is a supervised learning algorithm where key concept is based on the number of trees distributed randomly like a forest.[25,41] The learning accuracy of this algorithm is based on the number of trees present in the classification method. The larger is the number of trees, the greater will be the accuracy of prediction.[42,43] The trees represent the number of rule sets and these rules are used to perform the predictions. The major advantage of this technique is the limits of overfitting.[44,45] As the numbers of trees are limitless, so the classifier never over fits the model. Another advantage of this technique is that this model can handle missing values and the classifier can be tuned for categorical parameters.[45–47] The pseudo-code of the classification model and prediction process is shown below.

Developing random forest model.

Step 1: Select "K" numbers of features randomly out of "m" numbers of features where K≪m
Step 2: Calculate node "d" among "K" numbers of features
Step 3: Splitting of node into Daughter Nodes using best split approach
Step 4: Repeat the step 1 to 3 until "L" numbers of nodes has been obtained
Step 5: Repeat the step 1 to 4 to build forest having "N" numbers of trees

Developing prediction model.

Step 1: Consider the features and calculate the outcome from the decision tree
Step 2: Evaluate the "Votes" by estimating every predicted targets
Step 3: Consider only the highest voted predicted values as the final output of the model

4.4 | IoT decision support

The decision support model is developed and integrates with the proposed estimation model to generate adequate notifications for the city authority. The estimated load and position from the proposed prediction model is compared inside the decision model. The complete IoT decision support model consists of three broad functionalities such as detection, diagnosis, delivery, and so on. The detection functionality is the FBG sensing mechanism and estimation model; which produces load and position information to the diagnosis functionality. Furthermore, the diagnosis functionality contains rule-based modules to compare the estimated load with the threshold levels and generates case-based reasoning tokens.[48,49] These tokens are nothing but the key statements for the notifications. The final module is the delivery, which integrates the decision support model with the user application and application integration such as a web-based framework.[8–10] The proposed IoT decision support model to generate adequate notifications by integrating with user application software is shown in Figure 4.

5 | RESULTS AND DISCUSSION

The experimental analysis is performed on the prototype suspension bridge model by installing three FBG sensors. The steps followed during this experimental analysis are discussed in this

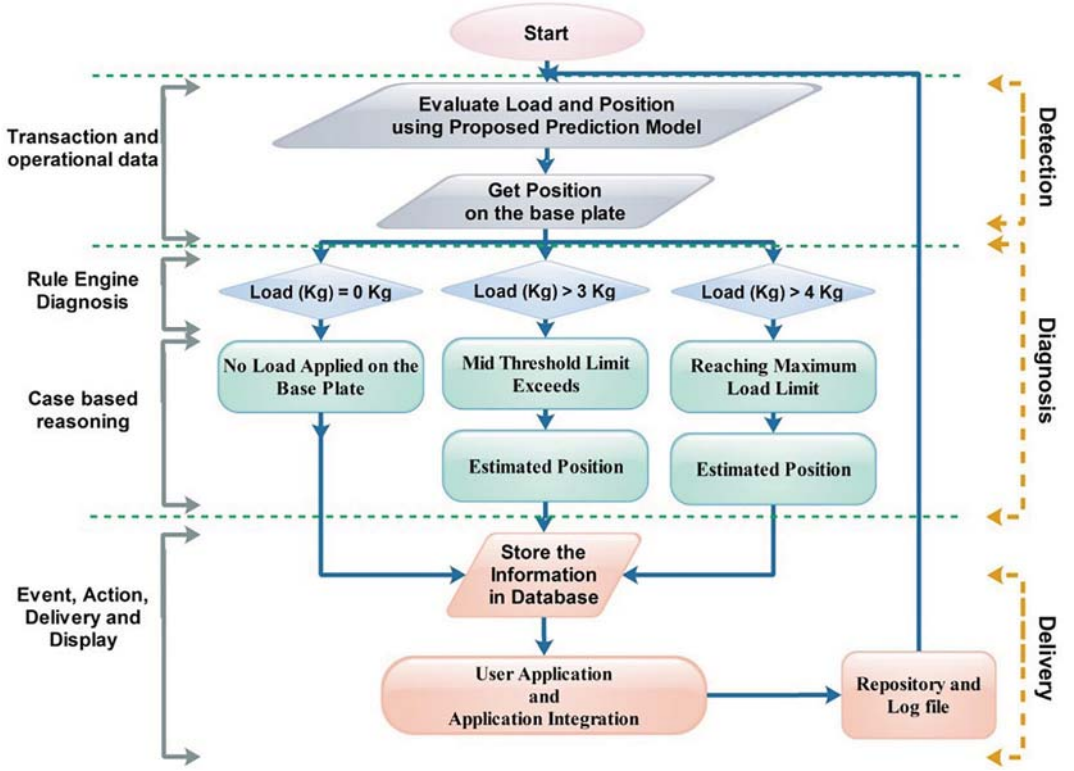

FIGURE 4 Decision support model to generate adequate notifications [Color figure can be viewed at wileyonlinelibrary.com]

section. First, the finite element analysis (FEA) of the structure is performed; and the maximum principal strain and maximum principal stress profile are evaluated using ANSYS software. Figure 5A,B shows the strain and stress distribution over the deck of the structure, respectively. It is observed from the FEA model is that the strain is maximum at two regions where the deck rests on the two vertical pillars.

The complete structure has three sections of 30.48 cm on both ends and 60.96 cm at the middle portion. Therefore, one-half length of the bridge structure (60.96 cm from one end) is sufficient to evaluate the real-time analysis of the load and position estimation using three FBG sensors.

Three FBG sensors are bonded on the deck plate to analyze the mathematical parameters observed from the FEA model and physical signals from the FBG Interrogator. The snapshot of the FBG sensors bonded on the deck of the suspension bridge model is shown in Figure 6A. The magnified portion of a single FBG sensor on the deck is shown in Figure 6B.

The FBG sensors are bonded as per their sensitive axis which is marked on the deck of the suspension bridge model. The broadband spectrum of the SLED source is shown in Figure 7. The real-time sensor signals are acquired using the FBG interrogator is shown in Figure 8. These are time-series signals with some noise components present due to optical losses present in the couplers, connectors, and external effects. As shown in Figure 8, the snapshot of the magnified portion of the unfiltered signal is quite significant and it is filtered using the proposed moving average filter.

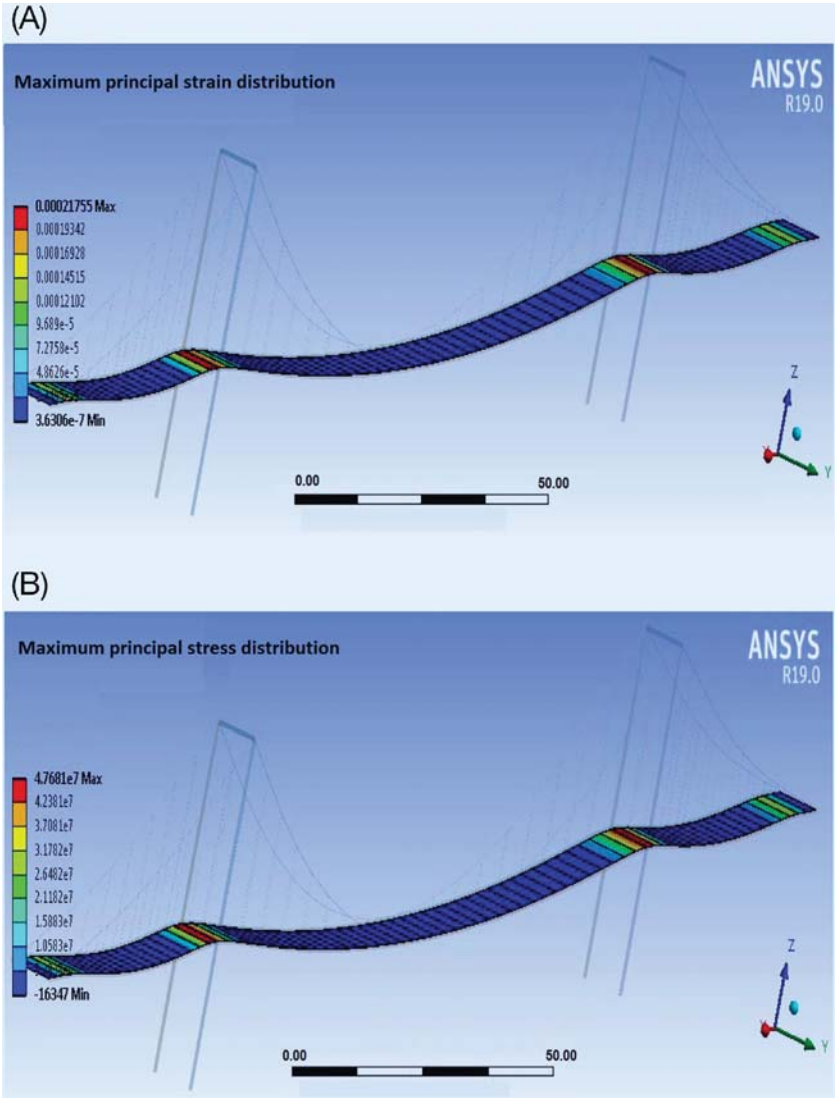

FIGURE 5 A, Maximum principal strain distribution. B, Maximum principal stress distribution [Color figure can be viewed at wileyonlinelibrary.com]

The unfiltered signals from the FBG sensors are filtered using the proposed moving average filter algorithm. The recorded response of the proposed filtering scheme is shown in Figure 9. The recording is taken from the IBSEN IMON FBG interrogator and Figure 9 shows the unfiltered with filtered signal together.

Furthermore, the load analysis is performed by applying standard weights at seven distinct positions marked on the deck from length (L = 0 cm) to the center position (L = 60.96 cm) of the deck. The signal recording using the IBSEN IMON FBG interrogator is discussed in Section 3 of this article. The signal recording is performed for the three FBG sensors and the wavelength shift concerning load, the position is plotted in Figures 10, 11, and 12. It is observed from the wavelength shift that the amplitude is minimum at the positions 3 and 7 for all the three FBG

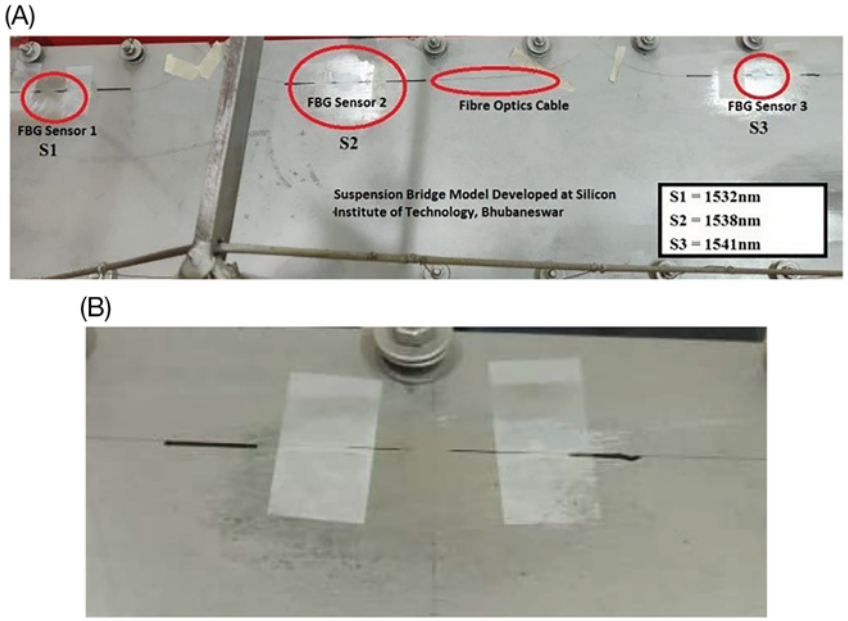

FIGURE 6 A, Three FBG sensors bonded on the deck of the suspension bridge. B, A magnified portion of a single FBG sensor bonded on the deck [Color figure can be viewed at wileyonlinelibrary.com]

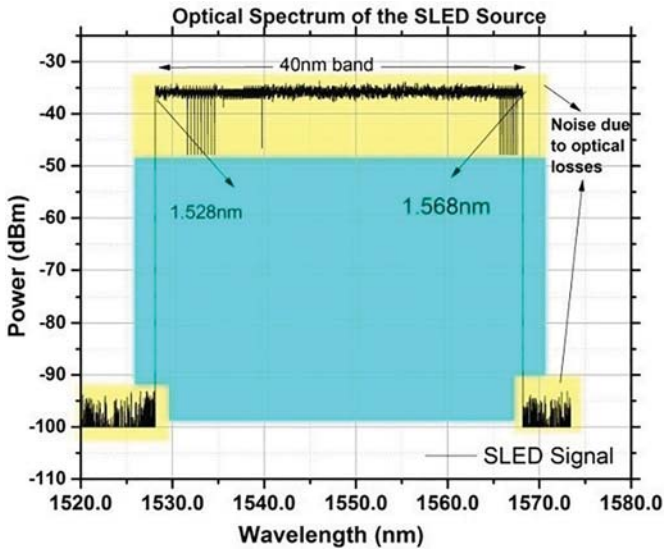

FIGURE 7 Optical spectrum of the SLED source (40 nm band) [Color figure can be viewed at wileyonlinelibrary.com]

sensors. This summarizes the placement of support pillars near those positions on which the deck rests by the suspension strings. This gives a virtual picture of the bridge structure and lower support of the deck.

Furthermore, the wavelength shift of three FBG sensors (S1, S2, S3) is used to tune the load and position estimation models such as K-nearest neighbor (KNN) and random forest (RF). The load and position estimation models are tested by evaluating the prediction errors such as MSE, RMSE, R-squared value, and accuracy. The comparative analysis between actual load (kg) and

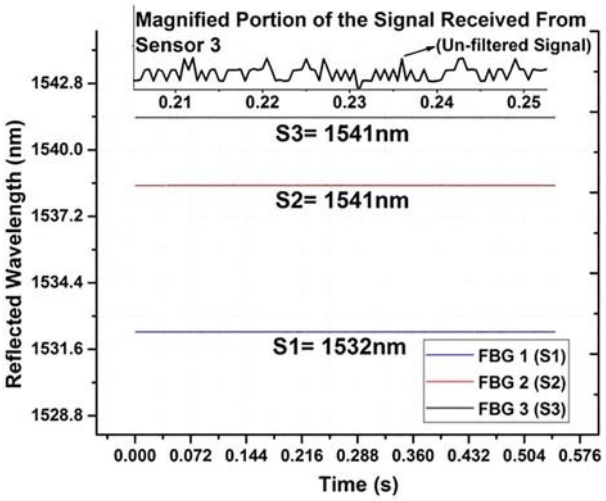

FIGURE 8 Unfiltered sensor signals from the IBSEN IMON FBG interrogator [Color figure can be viewed at wileyonlinelibrary.com]

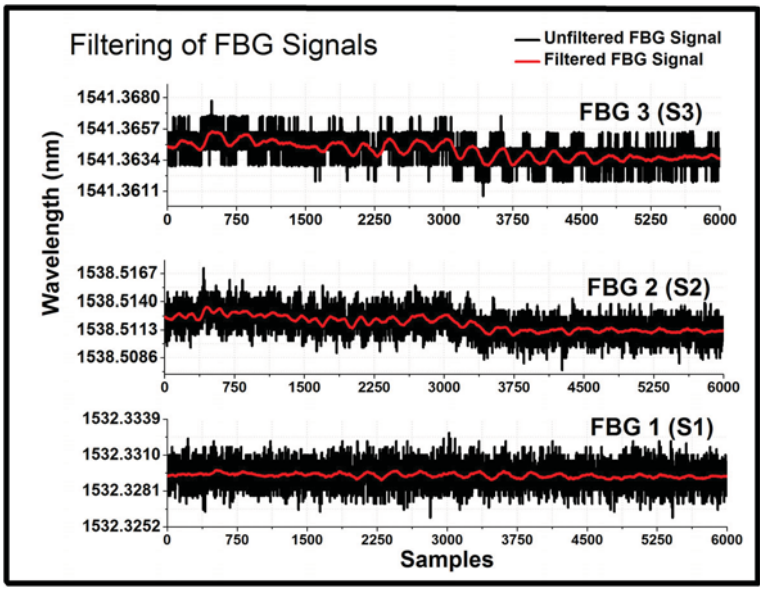

FIGURE 9 *Filtered sensor signals from the IBSEN IMON FBG interrogator* [Color figure can be viewed at wileyonlinelibrary.com]

estimated load (kg) for two proposed models is performed. Figure 13 shows the deviation from the actual load concerning the estimated loads using KNN and RF models. It is observed in Figure 13 that the KNN estimation model produces a much higher deviation from the actual load compared with the random forest (RF) based model. The error is quite higher from the applied load 2.5 to 4 kg in the case of KNN based model. The performance characteristics of the proposed soft sensing scheme are listed in Table 3. Furthermore, the load sensitivity at the predefined positions is found as 2.378272243 nm/g. Figure 12 also shows a magnified portion of such the highest deviation region.

Similarly, the position estimation is also performed using KNN and RF-based model; the prediction performance is shown in Figure 13. It is observed that the KNN-based position estimation

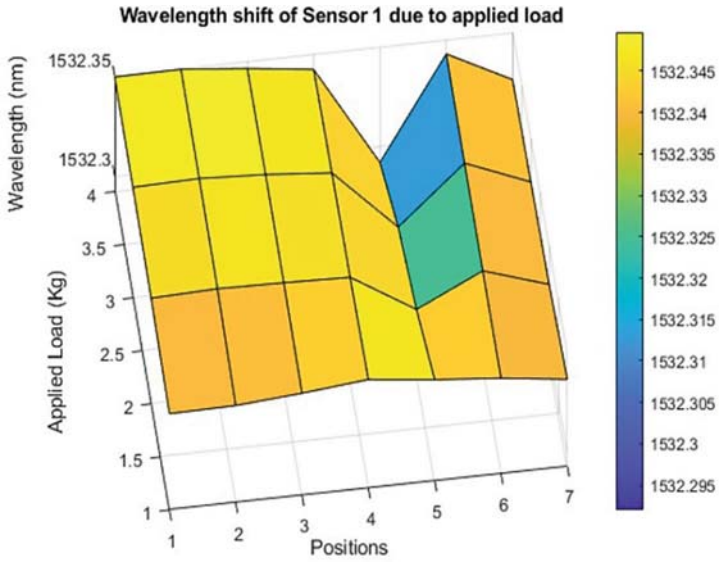

FIGURE 10 Wavelength shift of FBG sensor (S1) for different applied load at seven distinct positions [Color figure can be viewed at wileyonlinelibrary.com]

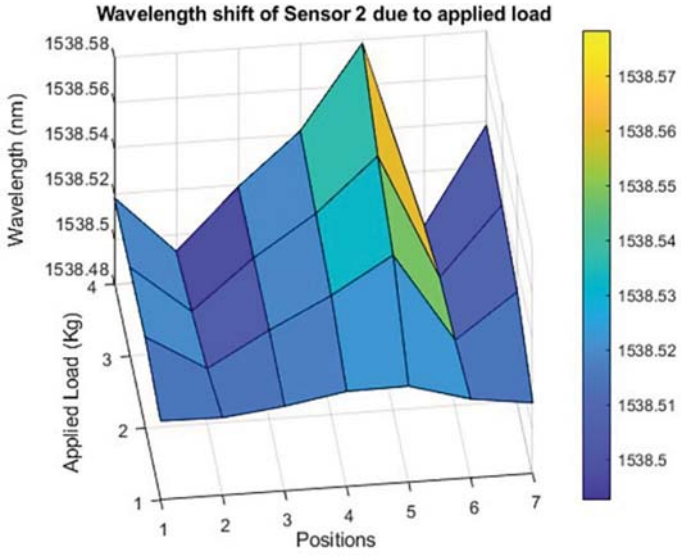

FIGURE 11 Wavelength shift of FBG sensor (S2)for different applied load at seven distinct positions [Color figure can be viewed at wileyonlinelibrary.com]

model produces the highest residual error compared with RF-based estimation. Figure 14 also shows the magnified portion of the maximum deviation from the actual positions.

The two proposed estimation models are analyzed and the performance analysis is also performed by evaluating prediction errors using MSE, RMSE, R-squared value, and accuracy. The errors and performance parameters are listed in Table 4 for both applied load and position.

It is observed that the accuracy of the random forest (RF) model is quite high compared with KNN-based model. The accuracy highest in the case of RF-based estimation and the errors are also lower compared with KNN.

Finally, the RF model is tested with known loads of 1 and 4 kg at position 3. The RF model accurately estimates the position 3 and applied loads. The estimated load and position are identified with the 3D view of the prototype suspension bridge model as shown in Figures 15 and 16.

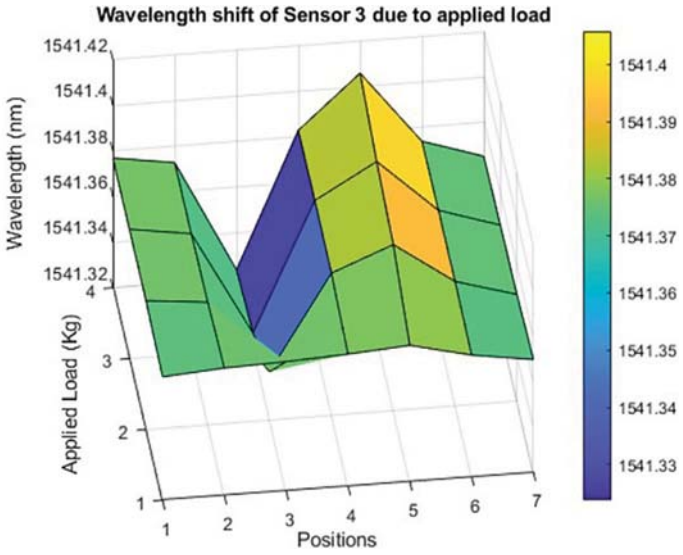

FIGURE 12 Wavelength shift of FBG sensor (S3) for different applied load at seven distinct positions [Color figure can be viewed at wileyonlinelibrary.com]

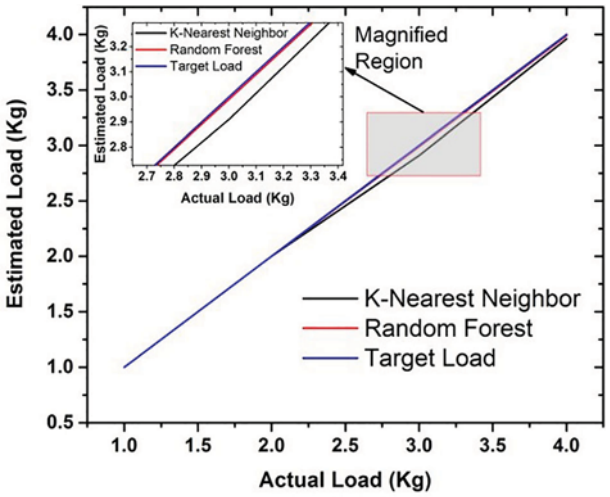

FIGURE 13 Performance of KNN and RF models for the estimation of applied loads (kg) [Color figure can be viewed at wileyonlinelibrary.com]

TABLE 3 Characteristics of the proposed soft sensing model

Characteristics	
Strain sensitivity (pm/με)	0.502623329
Load sensitivity at the test positions (pm/g)	2378.272243
Prediction accuracy of RF model for the applied load	95.9183%

It can be observed in Figures 15 and 16 that the red color intensity is increased with the increase in the applied load at position 3 on the bridge structure.

Finally, the IoT decision support model is developed and tested with different loads at predefined positions on the prototype suspension bridge structure. The test notifications generated from the decision support model are listed in Table 5. Finally, the web-based framework is developed using LabVIEW web GUI, which will be used by the authority for real-time

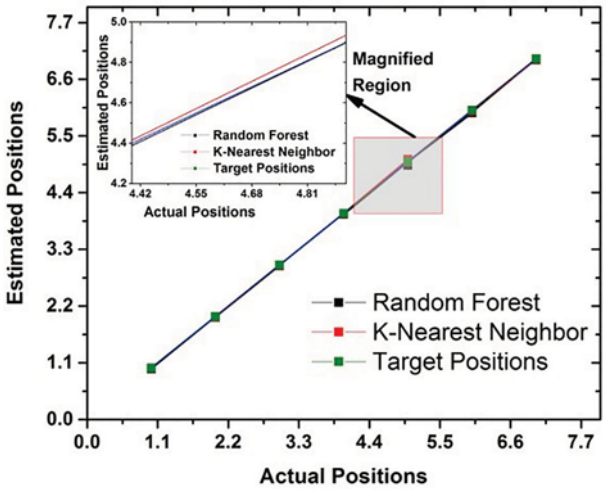

FIGURE 14 Performance of KNN and RF models for the estimation of positions [Color figure can be viewed at wileyonlinelibrary.com]

TABLE 4 Performance analysis of the load and position estimation models

Method	MSE	RMSE	R-squared	Accuracy	Remark
KNN (load estimation)	0.0816	0.2857	0.9231	91.8367	Low accuracy
KNN (position estimation)	0.5306	0.7284	0.8673	95.9183	Low accuracy
RF (load estimation)	0.0408	0.202	0.9615	95.9183	Good accuracy
RF (position estimation)	0.5306	0.7284	0.8673	95.9184	Good accuracy

FIGURE 15 3D view of the prototype suspension bridge model for 1 kg load applied at position 3 [Color figure can be viewed at wileyonlinelibrary.com]

FIGURE 16 3D view of the prototype suspension bridge model for 4 kg load applied at position 3 [Color figure can be viewed at wileyonlinelibrary.com]

TABLE 5 Test results of the developed GUI application

Sl no	Applied load (kg)	Position	Notification
1	0	1	No load applied on the deck at position 1
2	2	3	Midthreshold limit exceeds at position 3
3	4	5	Reaching maximum load limit at position 5

monitoring of the load flow on the bridge structure throughout the year. The snapshot of the web framework and notification generated using a test load input at position 1 is shown in Figure 17.

6 | CONCLUSION

FBG sensing technology is widely accepted in many SHM applications. Efficient signal processing, calibration, load prediction, and position localization in SHM application using FBG sensors is a challenging task. In this article, the proposed machine learning model based load and position estimation techniques such as KNN and RF models are implemented in the prototype suspension bridge structure.

6.1 | Findings

The load calibration is successfully implemented during this research and estimation errors are evaluated. Firstly, the load sensitivity at the predefined positions is obtained as 2.378272243 nm/g using the fabricated FBG sensors with the help of a femtosecond laser direct-writing system (femtoFBG writing system). Further, it is obtained that the load prediction and its position localization using the RF model produces minimum MSE of 0.0408 and 0.5306, respectively. On the other hand, the KNN based model produces much higher MSE of 0.0816 and 0.5306 for the prediction of the load as well as its position, respectively. Apart from that, it is also observed that three FBG sensors (1532, 1538, 1541 nm) are sufficient enough to predict the applied load and its position throughout the length of the bridge structure. In a similar context, the proposed technique shows the implementation of a soft sensing technique where three FBG sensors are sufficient to

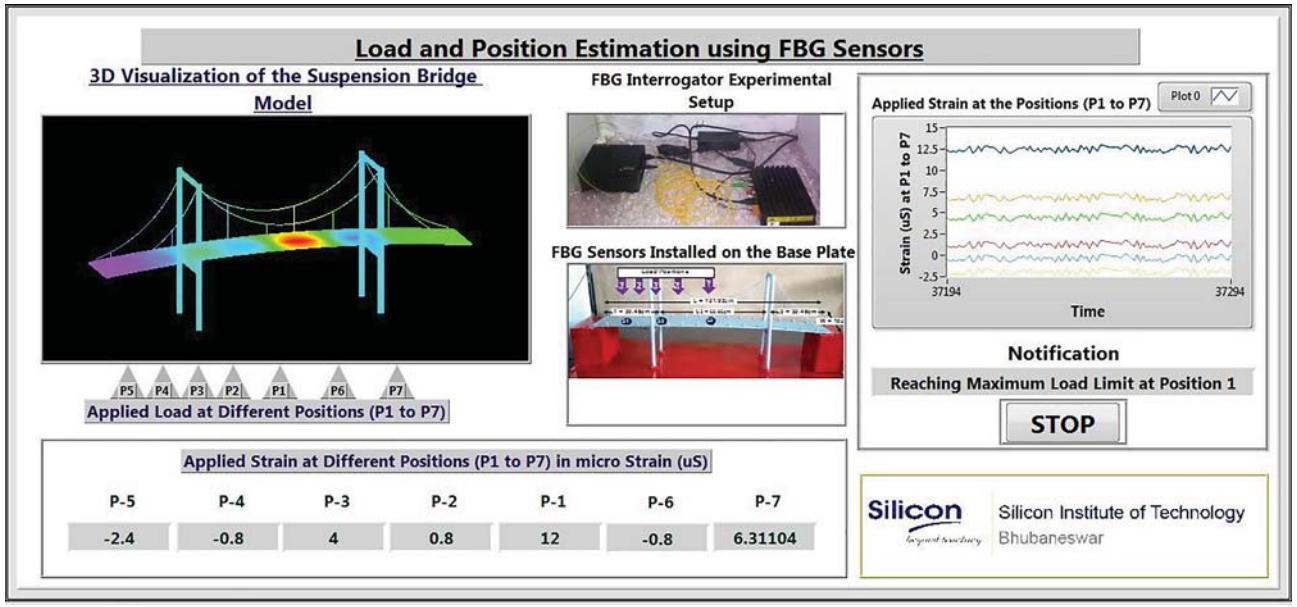

FIGURE 17 Web framework developed using LabVIEW Graphical Programming where position 1 is exposed to maximum strain [Color figure can be viewed at wileyonlinelibrary.com]

monitor the load distribution throughout the deck of the prototype suspension bridge model. The results show that the proposed RF model produces very good prediction accuracy for the applied load and its position to develop an IoT-driven visualization framework. This approach can be used to visualize the load at any point on a suspension bridge structure by installing commercial-grade FBG sensors and FBG interrogators in a real bridge structure. Finally, the IoT based Decision Support model is successfully implemented and tested with various test loads applied to predefined positions on the deck of the suspension bridge prototype structure.

ACKNOWLEDGMENTS

The authors thank Silicon Institute of Technology, Bhubaneswar, and Central Glass and Ceramic Research Institute (CGCRI), Kolkata to provide continuous support in fabricating the FBG sensors during the research work. The authors also thank Silicon Institute of Technology, Bhubaneswar to provide licensed software like LabVIEW and FBG interrogator application to conduct this experimental study. We would like to acknowledge the financial support received under the research project grant scheme TEQIP-III BPUT CRIS, Letter No. BPUT-XIX-TEQIP-III/17/19/119 Dated: 08/11/2019.

DATA AVAILABILITY STATEMENT

No data are available

ORCID

Ambarish G. Mohapatra https://orcid.org/0000-0001-5139-8889
Deepak Gupta https://orcid.org/0000-0002-3019-7161

REFERENCES

1. Rao YJ. In-fiber Bragg grating sensors. *Mea Sci Technol*. 1997;8:355-375.
2. Lima HF, da Silva Vicente R, Nogueira RN, et al. Structural health monitoring of the church of Santa Casa da Misericordia of Aveiro using FBG sensors. *IEEE Sens J*. 2008;8:1236-1242.
3. Reekie L, Chow YT, Dakin JP. Optical in-fibre grating high pressure sensor. *Electron Lett*. 1993;29(4):398-399.
4. Zhao Y, Zheng H-k, Lv R-q, Yang Y. A practical FBG pressure sensor based on diaphragm-cantilever. *Sens Actuat A*. 2018;279:101-106.
5. Williamson C, Fixter L. *State of the art review: structural health Monitoring*. NAMTEC and the Institute of Materials Minerals and Mining: London, UK: QinetiQ. QinetiQ/S&DU/T&P/E&M/TR0601122; 2006.
6. Mita A, Yokoi I. Fiber Bragg grating accelerometer for buildings and civil infrastructures, smart structures and materials 2001: smart systems for bridges, structures, and highways. Paper presented at: Proceedings of SPIE 4330; 2001.
7. Baldwin C, Niemczuk J, Kiddy J, Salter T. *Review of Fiber Optic Accelerometers, Systems Planning & Analysis*. Paper presented at: Proceedings of IMAC XXIII: A Conference & Exposition on Structural Dynamics, Orlando, FL : Micron Optics, Inc.; 2005: http://www.micronoptics.com/uploads/library/documents/fiberopticaccel.pdf.
8. Mohapatra AG, Lenka SK. Neuro-fuzzy-based smart DSS for crop specific irrigation control and SMS notification generation for precision agriculture. *Int J Converg Comput*. 2016;2(1):3-22.
9. Mohapatra AG, Keswani B, Lenka SK. Neural network and fuzzy logic based smart DSS model for irrigation notification and control in precision agriculture. *Proc Natl Acad Sci Section A Phys Sci*. 2018;6(24):1-10.
10. Keswani B, Mohapatra AG, Mohanty A, et al. Adapting weather conditions based IoT enabled smart irrigation technique in precision agriculture mechanisms. *Neural Comput Appl*. 2019;31:277-292. https://doi.org/10.1007/s00521-018-3737-1.
11. Rekha KS, Sreenivas TH, Kulkarni AD. Remote monitoring and reconfiguration of environment and structural health using wireless sensor networks. *Mater Today Proc*. 2018;5(1, Part 1):1169-1175.

12. Yasuda Shigeru, Miyazaki Shinya. Fatigue Crack Detection System Based on IoT and Statistical Analysis. *Procedia CIRP*. 2017;61:785–789. http://dx.doi.org/10.1016/j.procir.2016.11.260.
13. Amir HA, William GB. An overview of smartphone technology for citizen-centered, real-time and scalable civil infrastructure monitoring. *Future Gen Comput Syst*. 2019;93:651-672.
14. Mohanty SN, Ramya KC, Rani SS, et al. An efficient lightweight integrated blockchain (ELIB) model for IoT security and privacy. *Future Gener Comput Syst*. 2020;102:1027-1037.
15. Gochhayat Sarada Prasad, Lal Chhagan, Sharma Lokesh, Sharma D. P., Gupta Deepak, Saucedo Jose Antonio Marmolejo, Kose Utku. Reliable and secure data transfer in IoT networks. *Wireless Netw*. 2019. http://dx.doi.org/10.1007/s11276-019-02036-0.
16. Alzubi JA, Manikandan R, Alzubi OA, et al. Hashed Needham Schroeder IoT Based Cost Optimized Deep Secured Data Transmission in Cloud. *Measurement*. 2020;150:107077.
17. Patan R, Ghantasala GSP, Sekaran R, Gupta D, Ramachandran M. Smart healthcare and quality of service in IoT using Grey filter convolutional based cipher physical system. *Sustain Cities Society*. 2020;59:102141.
18. Chavhan Suresh, Gupta Deepak, Chandana B. N., Khanna Ashish, Rodrigues Joel J. P. C.. IoT-Based Context-Aware Intelligent Public Transport System in a Metropolitan Area. *IEEE Internet of Things*. 2020;7 (7):6023–6034. http://dx.doi.org/10.1109/jiot.2019.2955102.
19. Rodrigues R, Rodrigues JJPC, Cruz M, Khanna A, Gupta D. An IoT-based automated shower system for smart homes. Paper presented at: International Conference on Advances in Computing, Communications and Informatics (ICACCI'18); 2018. https://doi.org/10.1109/ICACCI.2018.8554793.
20. Mustapha S, Kassir A, Hassoun K, Dawy Z, Abi-Rached H. Estimation of crowd flow and load on pedestrian bridges using machine learning with sensor fusion. *Autom Construct*. 2020;112:1-17.
21. Bao Y, Chen Z, Wei S, Xu Y, Tang Z, Li H. The state of the art of data science and engineering in structural health monitoring. *Engineering* 2019;5:234-242.
22. Li R, Tan Y, Chen Y, Hong L, Zhou Z. Investigation of sensitivity enhancing and temperature compensation for fiber Bragg grating (FBG)-based strain sensor. *Opt Fiber Technol*. 2019;48:199-206.
23. Yu J. Dakai Liang, Xiaojing gong, Xuegang song, impact localization for composite plate based on detrended fluctuation analysis and centroid localization algorithm using FBG sensors. *Optik*. 2018;167:25-36.
24. Mieloszyk M, Ostachowicz W. An application of structural health monitoring system based on FBG sensors to offshore wind turbine support structure model. *Mar Struct*. 2017;51:65-86.
25. García R, Gimeno JM, Perdrix F, et al. Building a usable and accessible semantic web interaction platform. *World Wide Web*. 2010;13(1):143-167.
26. Sindagi VA, Patel VM. A survey of recent advances in cnn-based single image crowd counting and density estimation. *Pattern Recogn Lett*. 2018;107:3-16. https://doi.org/10.1016/j.patrec.2017.07.007.
27. Zhan B, Monekosso DN, Remagnino P, Velastin SA, Xu L-Q. Crowd analysis: a survey. *Mach Vis Appl*. 2008;19(5–6):345-357. https://doi.org/10.1007/s00138-008-0132-4.
28. Zhang Y, Zhou D, Chen S, Gao S, Ma Y, Single-image crowd counting via multicolumn convolutional neural network. Paper presented at: Proceedings of the IEEE Conference on Computer Vision and Pattern Recognition; 2016:589-597. doi:https://doi.org/10.1109/CVPR.2016.70.
29. Sindagi VA, Patel VM, CNN-based cascaded multi-task learning of high-level prior and density estimation for crowd counting, Paper presented at: 14th IEEE International Conference on Advanced Video and Signal Based Surveillance, Lecce, Italy; 2017:1-6. https://doi.org/10.1109/AVSS.2017.8078491.
30. Jiao L, Wu H, Bie R, Umek A, Kos A. Multi-sensor golf swing classification using deep CNN. *Proc Comput Sci*. 2018;129:59-65. https://doi.org/10.1016/j.procs.2018.03.046.
31. Alavi AH, Buttlar WG. An overview of smartphone technology for citizen-centered, real-time and scalable civil infrastructure monitoring. *Future Gener Comput Syst*. 2019;93:651-672. https://doi.org/10.1016/j.future.2018.10.059.
32. Li Xing-Xin, Ren Wei-Xin, Bi Kai-Ming. FBG force-testing ring for bridge cable force monitoring and temperature compensation. *Sens Actuat A*. 2015;223:105–113. http://dx.doi.org/10.1016/j.sna.2015.01.003.
33. Liang Minfu, Fang Xinqiu, Ning Yaosheng. Temperature Compensation Fiber Bragg Grating Pressure Sensor Based on Plane Diaphragm. *Photon Sens*. 2018;8 (2):157–167. http://dx.doi.org/10.1007/s13320-018-0417-9.
34. Tao Sicong, Dong Xiaopeng, Lai Bowen. Temperature-insensitive fiber Bragg grating displacement sensor based on a thin-wall ring. *Opt Commun*. 2016;372:44–48. http://dx.doi.org/10.1016/j.optcom.2016.03.092.

35. Allwood Gary, Wild Graham, Lubansky Alex, Hinckley Steven. A highly sensitive fiber Bragg grating diaphragm pressure transducer. *Opt Fiber Technol*. 2015;25:25–32. http://dx.doi.org/10.1016/j.yofte.2015.06.001.
36. He Jianping, Zhou Zhi, Ou Jinping. Simultaneous measurement of strain and temperature using a hybrid local and distributed optical fiber sensing system. *Measurement*. 2014;47:698–706. http://dx.doi.org/10.1016/j.measurement.2013.10.006.
37. Bhattacharya G, Ghosh K, Chowdhury AS. An affinity-based new local distance function and similarity measure for kNN algorithm. *Pattern Recognit Lett*. 2012;33(3):356-363.
38. Li Quanzhe, Shin SaeByuk, Hong Chung-Pyo, Kim Shin-Dug. On-body wearable device localization with a fast and memory efficient SVM-kNN using GPUs. *Pattern Recognit Lett*. 2017;1–11. http://dx.doi.org/10.1016/j.patrec.2017.10.005.
39. Xiao J. SVM and KNN ensemble learning for traffic incident detection. *Phys A Stat Mech Appl*. 2019;517(1):29-35.
40. Afuosi MB, Zoghi MR. Indoor positioning based on improved weighted KNN for energy management in smart buildings. *Energy Build*. 2020;212(1):109754.
41. JAVA Message Service. 2020 http://download.oracle.com/javaee/1.3/jms/tutorial/1_3_1fcs/doc/jms_tutorialTOC.html.
42. Breiman L. Random forests. *Mach Learn*. 2001;45(1):5-32.
43. Thenmozhi S, Thilagavathi P. Impact of agriculture on Indian economy, international research journal of agriculture and rural. *Development*. 2014;3(1):96-105.
44. Vitorino D, Coelho ST, Santos P, Sheets S, Jurkovac B, Amado C. A random forest algorithm applied to condition based wasterwater deterioration modeling and forecasting, 16th conference on water distribution system analysis (WDSA). *Proc Eng*. 2014;89:401-410.
45. Junga M, Tautenhahna S, Wirthb C, Kattgea J. Estimating basal area of spruce and fir in post-fire residual stands in Central Siberia using Quickbird, feature selection, and random forests, international conference on computational science (ICCS). *Proc Comput Sci*. 2013;18:2386-2395.
46. Kratzenberg M, Zürn HH, Revheim PP, Beyerb HG. Identification and handling of critical irradiance forecast errors using a random forest scheme—a case study for southern Brazil, European Geosciences Union general assembly (EGU). *Energy Proc*. 2015;76:207-215.
47. Patri A, Patnaik Y. Random forest and stochastic gradient tree boosting based approach for the prediction of airfoil self-noise, international conference on information and communication technologies (ICICT). *Proc Comput Sci*. 2015;46:109-121.
48. Ambarish G, Mohapatra SKL. Hybrid decision model for weather dependent farm irrigation using resilient Backpropagation based neural network pattern classification and fuzzy logic. *Proceedings of the Springer Smart Innovation, Systems and Technologies (SIST) Book Series, Chapter 30*. India: Springer; 2016:1-12.
49. Mohapatra AG, Lenka SK. Hybrid decision support system using PLSR-fuzzy logic for GSM based site specific irrigation notification and control in precision agriculture. *Int J Intell Syst Technol Appl*. 2016;15(1):4-18.
50. Koerdt M, Kibben S, Bendig O, et al. Fabrication and characterization of Bragg gratings in perfluorinated polymer optical fibers and their embedding in composite. *Mechatronics*. 2016;34:137-146.
51. Zheng R, Liu L, Zhao X, Chen Z, Zhang C, Hua X. Investigation of measurability and reliability of adhesive-bonded built-in fiber Bragg grating sensors on steel wire for bridge cable force monitoring. *Measurement*. 2018;129:349-357.

How to cite this article: Mohapatra AG, Khanna A, Gupta D, Mohanty M, de Albuquerque VHC. An experimental approach to evaluate machine learning models for the estimation of load distribution on suspension bridge using FBG sensors and IoT. *Computational Intelligence*. 2020;1–23. https://doi.org/10.1111/coin.12406